

Zicheng Deng¹, Donglu Shi², Vladimir V Kalinichenko^{1,3}
¹ Phoenix Children's Health Research Institute, Department of Child Health, University of Arizona College of Medicine-Phoenix
² The Materials Science and Engineering Program, College of Engineering and Applied Science, University of Cincinnati,
³ Division of Neonatology, Phoenix Children's Hospital

Background

Endothelial dysfunction contributes to a wide range of severe pulmonary vascular diseases such as Pulmonary hypertension, pneumonia, idiopathic pulmonary fibrosis, cystic obstructive pulmonary disease, bronchopulmonary dysplasia (BPD) and alveolar capillary dysplasia with misalignment of pulmonary veins (ACDMPV). The transcription factor FOXF1 plays a key role in pulmonary vascular development and endothelial repair after lung injury. Mutations in the FOXF1 gene has been associated with lung ACDMPV, a fatal congenital lung disorder, hypoplasia, and paucity of alveolar capillaries in newborns and infants. Nanoparticle delivery of FOXF1 has promise for ACDMPV treatment. However, there is still a critical need for versatile platforms that can deliver gene payloads and drugs to pulmonary endothelium with high efficiency and precision. The clinical translations of viral vectors are limited by their high biosafety risks. While several nanoparticle delivery systems have been recently developed, but none of them are specific to lung endothelial cells without targeting other cell types and organs. To treat pulmonary vascular disorders via gene therapy, it is necessary to develop a novel nanoparticle delivery system.

Design

This study focuses on the development of nanoparticle systems for efficient and precise delivery of nucleic acids to endothelial cells, particularly in pulmonary diseases. We developed a facile synthesis of the polymer with hydrophobic PBAE backbones and capped with the hydrophilic low molecular polyethylenimine (PEI) and poly (ethylene glycol) (PEG). This amphiphilic structure provides excellent nanoparticle colloidal stability and cationic density for gene encapsulation and delivery. Furthermore, we used fluororous ligands to improve the performance of the PBAE nanoparticles and achieve lung-specific delivery via the systemic intravenous route.

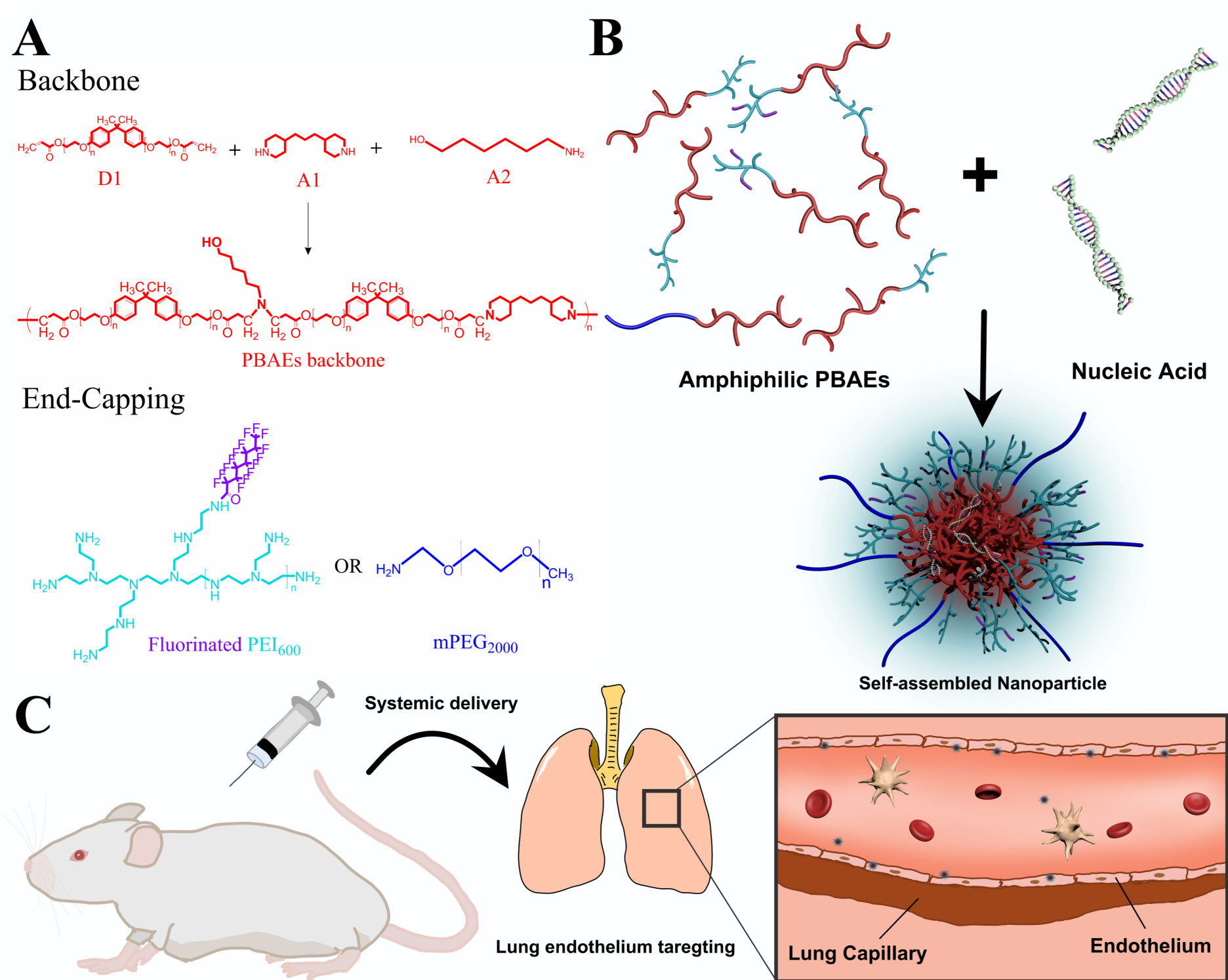
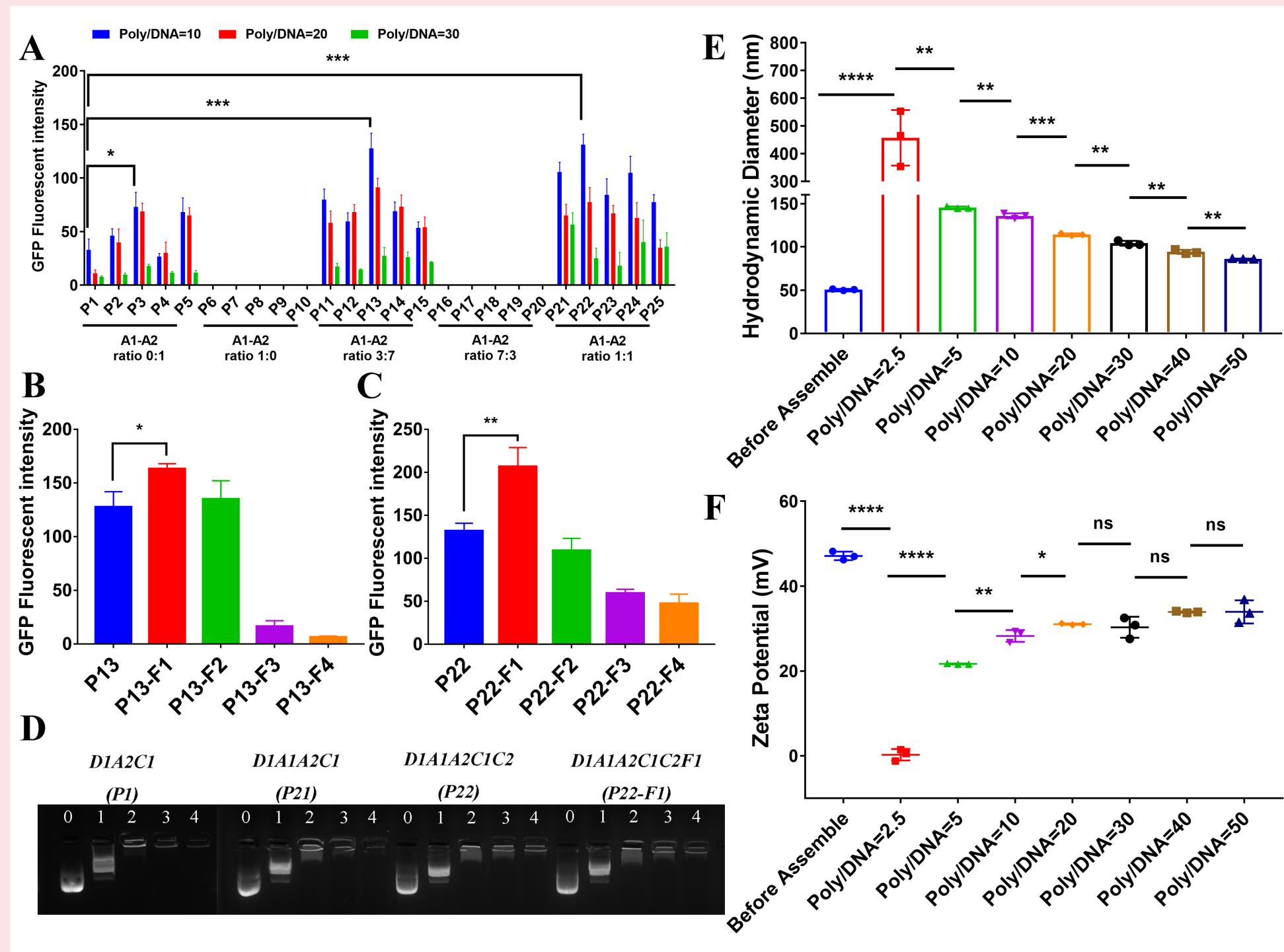
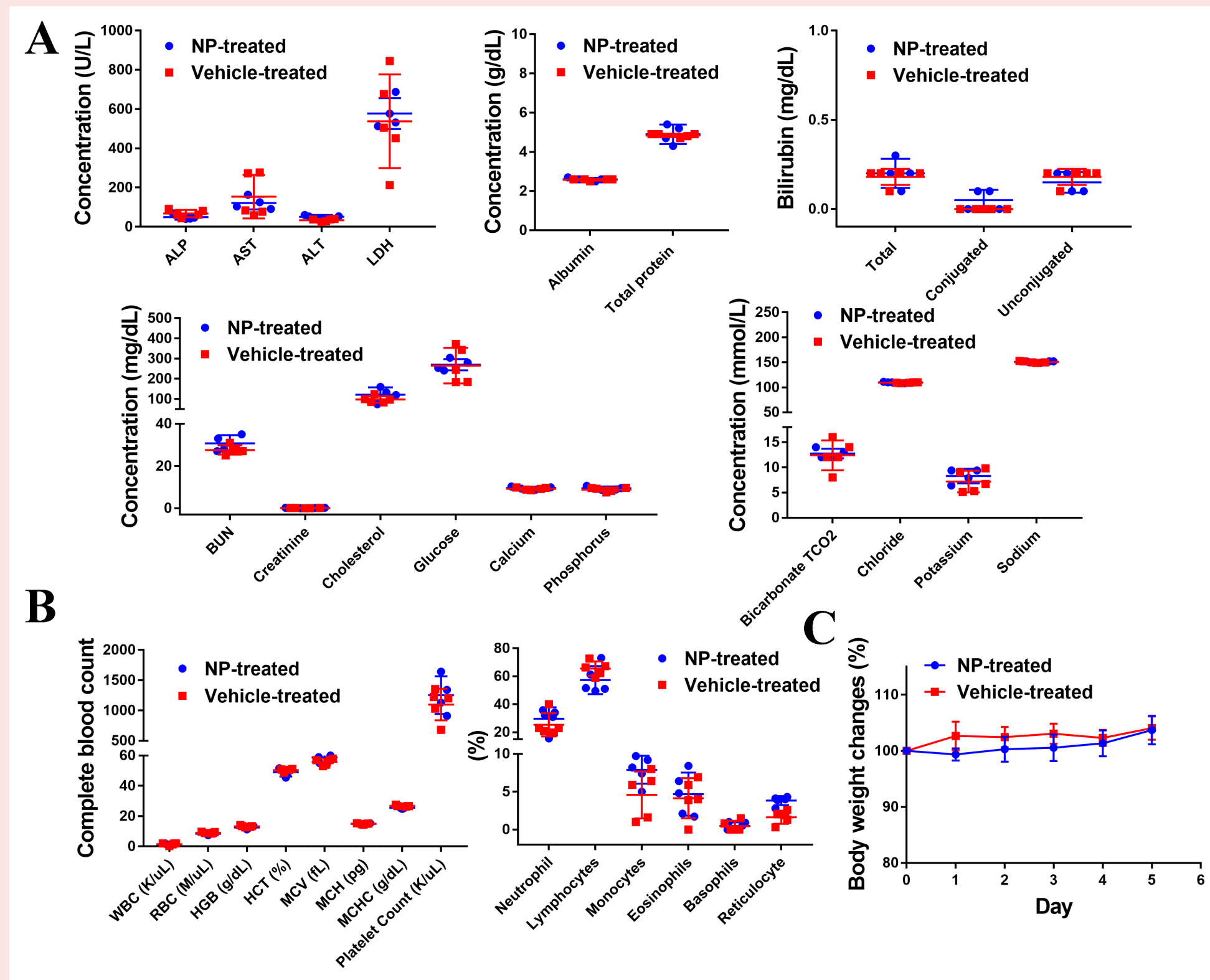


Figure 1. Overview of the PBAE nanoparticle synthesis and gene delivery to the pulmonary endothelium.

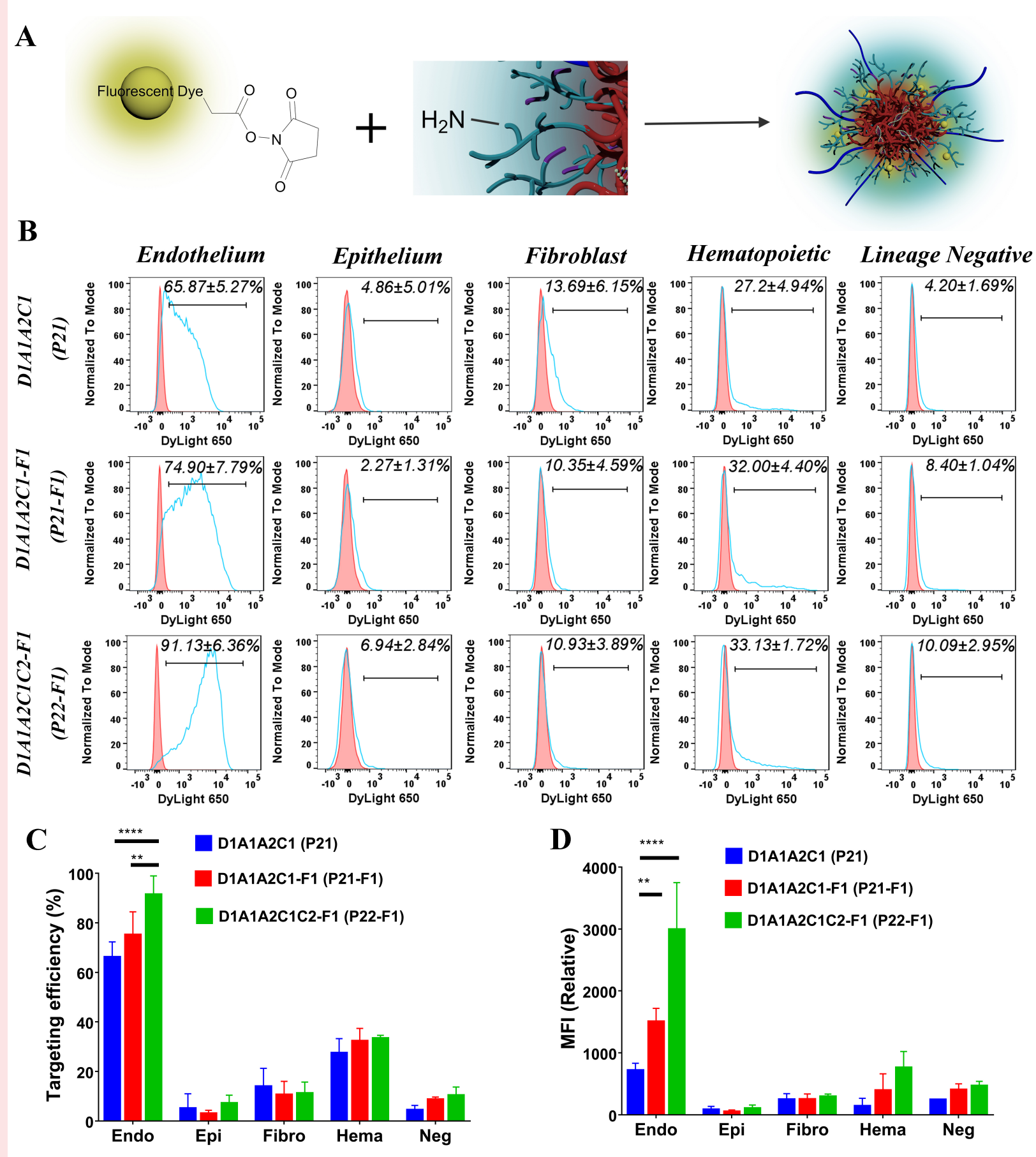
RESULTS



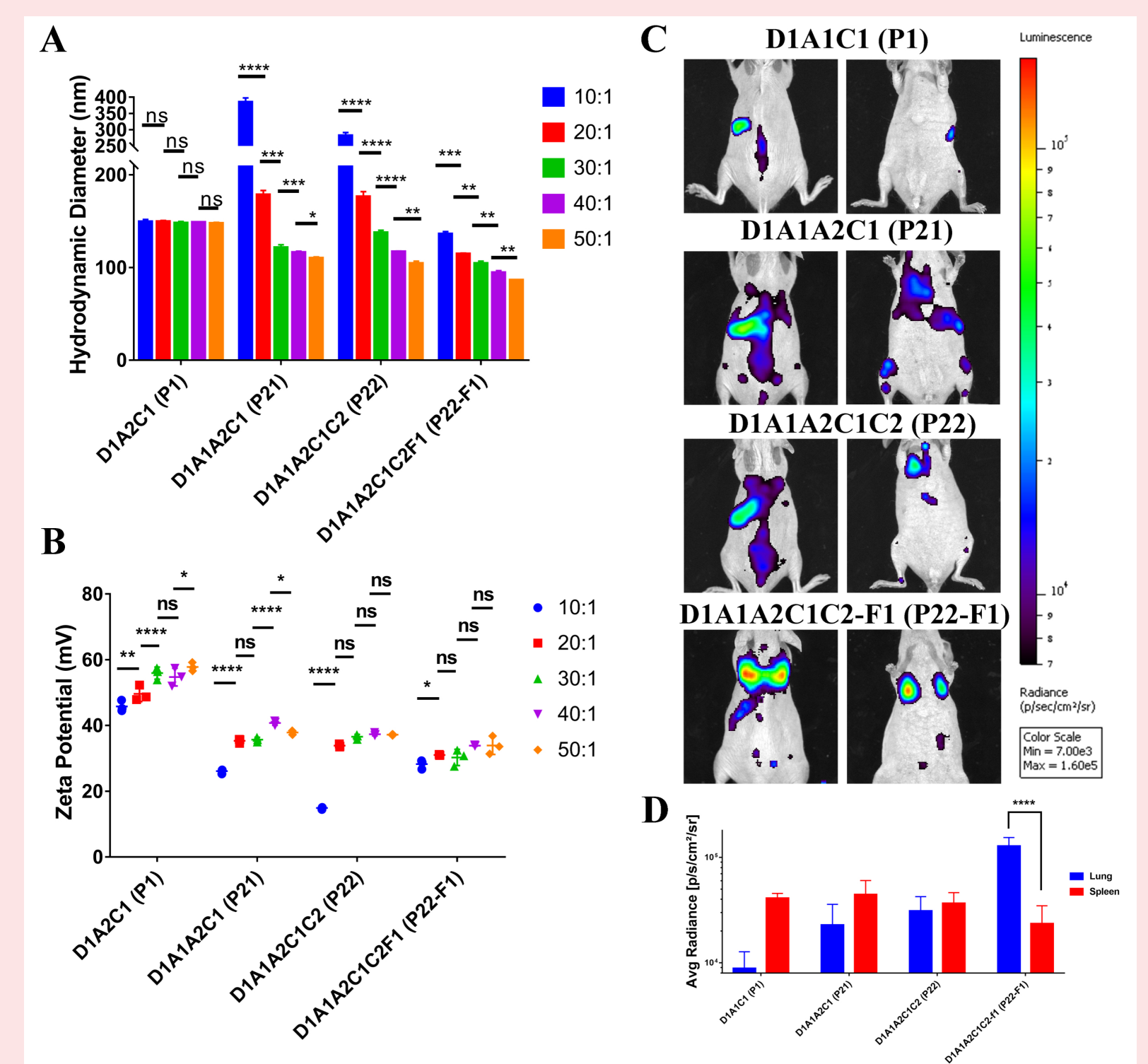
The effect of fluorination of PBAE polymer on the size, charge and transfection efficiency of the nanoparticles. (A) *In vitro* transfection efficiency of PBAE nanoparticles with different formulations and polymer to DNA mass ratios. (B) The influence of fluororous ligands on the *in vitro* transfection efficiency of the PBAE P13. (C) The influence of fluororous ligands on the *in vitro* transfection efficiency of the PBAE P22. (D) Gel electrophoresis analysis of plasmid DNA bound to the PBAE P1, P21, P22 and P22-F1 at different polymer to DNA mass ratios. (E) The hydrodynamic diameter of the PBAE P22-F1 nanoparticles at different polymer to DNA mass ratios. (F) The zeta potential of the PBAE P22-F1 nanoparticles at different polymer to DNA mass ratios.



Toxicity studies of the P22-F1 PBAE nanoparticles. The peripheral blood was collected from mice 5 days after a single intravenous injection of the P22-F1 PBAE nanoparticles. (A) The peripheral blood was assayed for major parameters in clinical chemistry, including those related to the liver and kidney metabolic panels, n = 5 mice per group. (B) Major parameters in hematology after analysis of peripheral blood. (C) Body weight changes after nanoparticle treatment.



The P22-F1 PBAE nanoparticles exhibit improved endothelial targeting in the lung tissue. (A) Fluorescent dye labeling of PBAE nanoparticles. (B) Flow cytometry analysis of the PBAE nanoparticle distribution (blue curve) in different respiratory cell types compared to the control (red curve). (C) Juxtaposition of cell targeting efficiency from P21, P21-F1 and P22-F1 PBAE nanoparticles (n = 3 mice were used for each group), $P < 0.0001$ is ****, $P < 0.01$ is **. (D) Juxtaposition of MFI from respiratory cells targeted with P21, P21-F1 or P22-F1 PBAE nanoparticles (n = 3 mice were used for each group), $P < 0.0001$ is ****, $P < 0.01$ is **. Abbreviations: Endo: Endothelium; Epi: Epithelium; Fibro: Fibroblast; Hema: Hematopoietic; Neg: Lineage negative



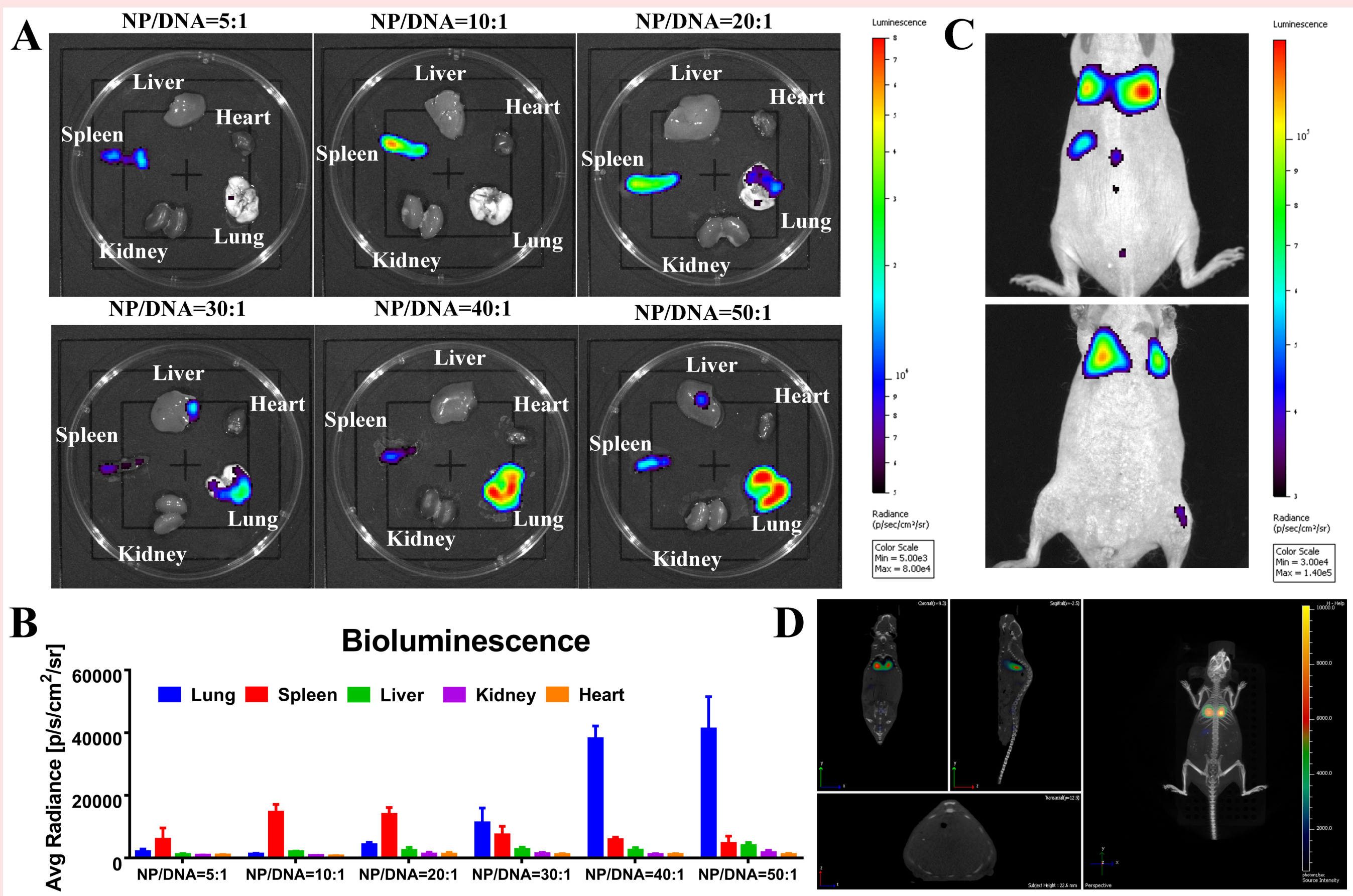
Fluorination influences *in vivo* biodistribution of the PBAE nanoparticles. (A) The hydrodynamic diameter of D1A2C1(P1), D1A1A2C1(P21), D1A1A2C1C2(P22), and D1A1A2C1C2F1 (P22-F1) nanoparticles at different NP/DNA mass ratios. (B) The zeta potential of D1A2C1(P1), D1A1A2C1(P21), D1A1A2C1C2(P22), and D1A1A2C1C2F1 (P22-F1) nanoparticles at different NP/DNA mass ratios. (C) Bioluminescence imaging shows distribution of D1A2C1(P1), D1A1A2C1(P21), D1A1A2C1C2(P22), and D1A1A2C1C2F1 (P22-F1) nanoparticles in mice. (D) Bar graph shows the quantification of luminescence in the lung and spleen. ns is not significant, * is $P < 0.05$, ** is $P < 0.01$, *** is $P < 0.001$, **** is $P < 0.0001$

DISCUSSION

The PBAE polymer synthesis was found to be sensitively controlled by the A1 to A2 ratio for optimum transfection efficiencies. It is likely that the underlying mechanism of the A1 to A2 ratio effects is related to the hydrophobicity of the monomers on the polymer backbones in order to form stable nanoparticles in gene delivery. PEG has been widely used in NPs synthesis to improve NPs stability, increase circulation time *in vivo*, and reduce toxicity. In this study, the addition of PEG at 3%-6% in the end caps was found to increase the transfection efficiency. However, further increasing the PEG ratio in end caps reduced transfection. Fluorination by F1 can further increase the transfection efficiency. Interestingly, *in vivo* luciferase imaging demonstrated that at low NP/DNA ratio of 10, the nanoparticles have a relatively large size, and the transfection occurs mainly in the spleen. With the increase of NP/DNA ratio to 50, the size of the nanoparticles was reduced dramatically, changing bioluminescence distribution in which the lung becomes the major targeted organ. The transfection patterns and organ specificity of NPs *in vivo* can be controlled by modifying the backbone structures of the NPs, adjusting the contents of capping agents, and optimizing the polymer-to-nucleic acid ratio. Our results consistent with published studies demonstrated that the size of the nanoparticles is important for its *in vivo* fate. Glycocalyx on the surface of endothelial cells is negatively charged, The P22-F1 NPs exhibit an inherent attraction or affinity towards endothelial cells, due to their positively charged surfaces. Importantly, hematologic analysis and liver/kidney metabolic panels confirmed the nanoparticles' non-toxic nature.

CONCLUSIONS

In conclusion, we have developed a facile synthesis of amphiphilic PBAE nanoparticles for pulmonary endothelial specific targeting and effective delivery. The transfection efficiency of PBAE nanoparticles can be optimized by changing the ratio of two alkyl chains in the backbones. The addition of PEG and fluorination can further increase the transfection of the NP. At low NP/DNA ratios, the transfection occurred only in the spleen, but the lung became the primary targeted organ after increasing the NP/DNA ratio. And the Nanoparticle is non toxic, and can maintain lung specificity even in the presence of neonatal lung injury. Overall, fluorinated PBAE nanoparticles offer a promising platform for gene therapy targeting lung microvascular endothelium in pulmonary vascular disorders.



In vivo transfection studies of P22-F1 PBAE nanoparticles. (A) Luminescent images show the biodistribution of luciferase expression at different nanoparticle to DNA ratios (10:1; 20:1; 30:1; 40:1, and 50:1) in dissected mouse organs. (B) Quantification of luminescence from different organs (n = 3 mice per group); (C) IVIS whole-body imaging shows the *in vivo* bioluminescence following treatment with P22-F1 PBAE nanoparticles. Ventral (top) and dorsal (bottom) view of the mouse are shown. (D) MicroCT images show the bioluminescence in the lung of mice treated with P22-F1 PBAE nanoparticles.